SINERGI Vol. 28, No. 3, October 2024: 595-604
http://publikasi.mercubuana.ac.id/index.php/sinergi
http://doi.org/10.22441/sinergi.2024.3.015

Improvement of ankle foot orthotics fabrication using 3D printing method

Kushendarsyah Saptaji[1]*, Dinda Arina Manasikana[1], Octarina Adiati Juniasih[2], Mochammad Rafli Ramadhani[1], Muchammad Oktaviandri[3], Anwar Ilmar Ramadhan[4], Yuli Panca Asmara[5]
[1]Mechanical Engineering Department, Faculty of Engineering and Technology, Sampoerna University, Indonesia
[2]Department of Mechanical Engineering, Sepuluh Nopember Institute of Technology, Indonesia
[3]Department of Mechanical Engineering, Universitas Pembangunan Nasional Veteran, Indonesia
[4]Department of Mechanical Engineering, Universitas Muhammadiyah Jakarta, Indonesia
[5]Faculty of Engineering and Quantity Surveying, INTI International University, Malaysia

Abstract
Orthotics are the body support devices used for correction, immobilization, fixation, and prevention of paralysis. The greatest number of orthotics utilized by people suffering from plantarflexion and dorsiflexion disability, especially in Indonesia, is ankle foot orthotic (AFO). However, the duration associated with fabricating AFO through conventional methods is considered time-consuming. This paper aims to fabricate ankle foot orthotics (AFO) using innovative combinations of 3D scanning and 3D printing. The method begins with 3D scanning of the patient's lower limb using photogrammetry (3DF Zephyr). The design is generated and adjusted, afterwards, the orthotic prototype is produced by fused deposition modeling (FDM) 3D printing using polypropylene (PP) material. This choice is attributed to the material's advantages, such as being lightweight, rigid, durable, and cost-effective. The 3D mesh model scanned using 3DF Zephyr shows good quality and more precise results. In addition, the prototype produced using 3D printing was tested by walking based on normal gait analysis's angle of foot and calf measurement, which shows a maximum range of motion (ROM) of 16.1˚. The proposed methods of fabricating orthotic prototypes can successfully reduce the processing time by approximately 70% compared to the conventional method.

Keywords:
3D scanning;
3D printing;
Ankle-foot orthotics (AFO);
Gait Cycle;
Photogrammetry;

Article History:
Received: December 11, 2023
Revised: February 22, 2024
Accepted: March 12, 2024
Published: October 2, 2024

Corresponding Author:
Kushendarsyah Saptaji
Mechanical Engineering Department, Faculty of Engineering and Technology, Sampoerna University, Indonesia
Email: kushendarsyah@sampoernauniversity.ac.id

INTRODUCTION

According to the World Health Organization (WHO), approximately 15% of the global population lives with some form of disability. In Indonesia, a report by Monash University estimates that at least 10 million people have disabilities, representing about 4.3% of the population. The data also highlights that one of the most common health conditions affecting daily functioning is lower limb disabilities. [1]. These disabilities may result from illnesses, accidents, or congenital conditions. An orthosis serves as a specialized orthopedic device designed to correct, accommodate, or enhance the function of a body part that has lost its functionality. It either aids or prevents the movement of a limb or the spine, categorizing it as a crucial biomedical device [2]. Furthermore, the lower limb plays a pivotal role in providing support for body movement [3].

Ankle-foot orthosis (AFO) is the most commonly prescribed lower limb orthotics. It is customized for individuals with walking-related functional limitations due to weakened ankle musculature and paralysis. AFOs play a pivotal role in modulating the gait cycle by providing external support, control, and stability to the ankle and foot. Therefore, the presence of AFO could support the ankle motion during the gait

cycle [4]. Gait cycle refers to a fundamental aspect of human locomotion, encompasses the repetitive events of walking and running, begins when one-foot contacts the ground and ends when the same foot contacts the ground repeatedly [5]. By aligning and supporting the lower extremities, AFOs contribute to the optimization of the gait cycle, assisting individuals in achieving a more natural and efficient walking pattern.

AFO traditional manufacturing processes are handcrafted by orthopedists which involves direct patient interaction during casting and fitting sessions [6], allowing for real-time adjustments based on patient feedback. However, this crafting method required skilled orthotist since the product quality depends on the specialist skills and experience [7]. In addition, AFOs fabrication using conventional methods involves a series of time-consuming processes. These typically include patient assessment, manual casting, material selection, molding and shaping, adjustments, and a finalization phase. This method required longer processing time, higher costs, and may generate more material waste [8]. Other than that, the traditional method such as casting process has low dimensional accuracy [9], resulting in a low geometrical representation of the model.

Alternatively, orthotic devices can be revolutionized in their production through the implementation of additive manufacturing (AM) technology also known as 3D printing. This cutting-edge technology capable of accelerates production time while maintaining high degree of precision [10]. Presently, fused deposition modelling (FDM) printing stands out for its ease of implementation and compatibility with common thermoplastic materials [11]. Moreover, the use of FDM is applicable for AFO due to its results of the porosity and density measurement [12]. Besides, it has demonstrated its capability to produce parts with complex geometrical features which makes FDM attractive for AFO manufacturing [13].

The incorporation of this manufacturing method with 3D scanning technology enables the fabrication of patient-specific anatomical models based on image data [14]. Scanning method collectively gathered the foot's accurate dimension and morphology for constructing 3D model of the AFO device [15]. By utilizing Computer-Aided Design (CAD) software, the 3D scan undergoes detailed processing, allowing for precise adjustments to the geometry [9]. Subsequently, the refined orthotic design 3D model can be seamlessly exported for production using a 3D printer. Therefore, this technology continues to advance, promoting a new era of patient-specific, efficient, and customized solutions in the medical field [16][17].

Apart from the fabrication process, the quality and the mechanical property of the prototype is also crucial [18]. Since the orthoses are produced to meet the specific function based on the user's needs, the presence of finite element analysis (FEA) specifically the stress-strain analysis becomes essential [19]. This analysis helps in predicting the prototype's ability to withstand the user's weight and prevent material failures [20][21]. It is possible to examine the mechanical behavior of AFO parts under certain loading and boundary conditions according to the patient requirement [22].

Regarding the background mentioned, the development of lower limbs orthotics fabrication process has been pursued. It is focused on transitioning conventional manufacturing methods to the additive manufacturing process, offering increased ease, flexibility, and accelerated fabrication capabilities. The objective of this study is to fabricate and assess the reliability and efficiency of AFO prototype. The fabrication process employed photogrammetry method which delivers a 3D image by combining multiple photos of the specific object. Photogrammetry scanning presents a groundbreaking alternative to traditional 3D scanning techniques by utilizing photographs taken with smartphone cameras. This approach simplifies the scanning process, making it more accessible and user-friendly. With just a series of photographs captured from different angles, photogrammetry can generate detailed 3D models, eliminating the need for specialized 3D scanner machines. This innovative method can be effectively employed in scanning patient's foot to customize the AFO design. Furthermore, the captured data can be processed remotely, enabling long-distance customization, and enhancing efficiency in patient care. Afterwards, the 3D design and 3D printed prototype were analyzed using FEA and gait cycle analysis. Understanding the gait cycle helps in optimizing the function of the AFO throughout the different phases of walking. It is expected that this method can produce an Ankle Foot Orthotic prototype suitable for patients with more effective production time compared to conventional methods.

METHOD

In this study, the ankle-foot orthotics fabricated manufactured to address the unique biomechanical needs and anatomical

characteristics of the individual by implementing 3D scanning and 3D printing method. This approach ensures a better fit and enhances the effectiveness of the AFO in providing support for the user. Therefore, it could increase the precision and individualization in the development of orthotic solutions within the study. The method is divided into four main steps: scanning and designing, FEA, fabrication, and evaluation processes.

Scanning and Designing Process

The alternative 3D scanner object photogrammetry was used in this study since constructing the 3D laser scanner is typically very expensive. The photogrammetry applications employed to obtain the 3D model are Meshroom and 3D Zephyr. These two photogrammetry applications also provide the simplest process compared to other applications. Moreover, the result of photogrammetry scanning process is a 3D mesh and still required further processing stages such ad editing and refining. The editing process of the 3D model is conducted by converting the mesh to solid feature using SolidWorks software.

Finite Element Analysis Process

Once the solid model is completed and verified, finite element analysis (FEA) was performed. The FEA was conducted in order to evaluate the strength of the ankle foot orthotics design. The model was then divided into smaller bodies or FE (Finite Element) and interconnected at a common point is called discretization [23]. SolidWorks software was employed to execute the FEA of the model. The analysis can be done by projecting every part of the AFO which was done by divided into some parts of the foot.

Fabrication Process

The ankle foot orthotics model was fabricated using a 3D printing process. FDM was chosen due to its cost-effectiveness and compatibility for a wider range of polymers. Additionally, it enables the production of customized and complex geometries that might be challenging to fabricate. In this specific method, polypropylene (PP) is considered suitable for orthoses applications due to its cost, quality, toughness and rigidity [6]. PP is practical for Ankle-Foot Orthoses with Flexural modulus of 190,000 psi (per-ASTMD790). Besides, it almost used in every types of conventional orthotics with printing temperature in the range of 240-260˚C [24][25]. Moreover, the fabrication parameter of the AFO is always based on the patient foot. Therefore, the parameter details can be shown after the 3D scanning and scaling processes.

Evaluation

One of the goals of this study is also to fabricate an AFO prototype which is safe and comfortable during standing or walking activities. Hence, the prototype testing performed through patient fitting in accordance with the normal gait cycle [26] where it includes seven stages. Those seven stages are heel strike, load response, midstance, terminal stance, initial swing & mid swing, and terminal swing. Gait cycle was also related to the range of motion (ROM) of the ankle. In this study, ROM is considered crucial for optimal weight distribution and balance during activities such as standing, walking, or running. For lower-extremities, ROM stands for the extend or limit of foot ankle to move around the ankle joint or simply the sum of dorsiflexion a plantar flexion. Dorsiflexion means the flexion of the foot upward while the plantar flexion is the opposite. The ankle neutral angle as the reference in gait cycle motion is 90°. For normal adult men, the maximum angular deviations range of the dorsiflexion is 10° to 15°, and for plantar flexion is 40° to 55°. However, during everyday activities, the maximum ROM in the sagittal plane for walking is 30° [27].

For medical devices like AFOs, patient comfort and rehabilitation timelines are crucial. A faster fabrication process means shorter wait times for patients, contributing to improved overall healthcare outcomes. Therefore, the time effectiveness analysis was conducted in order to assess the 3D printed AFO compared to conventional fabrication method.

RESULTS AND DISCUSSION

Designing Result Process

In order to develop the ankle foot orthotics model, a dummy patient of lower limb part was scanned. The 3D scanning process of the body part was similar to scanning process of non-living object. Figure 1 shows the patient injured lower limb (left) and the result of 3D scanning using 3DF Zephyr. The 3DF Zephyr works by rendering the photos taken. The figure shows a 3D model of the legs including the calf. Therefore, the 3D design of AFO can be generated based on this 3D model.

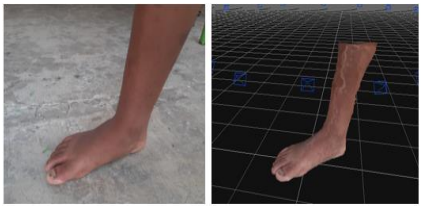

Figure 1. 3D Scan of lower limb using 3DF Zephyr

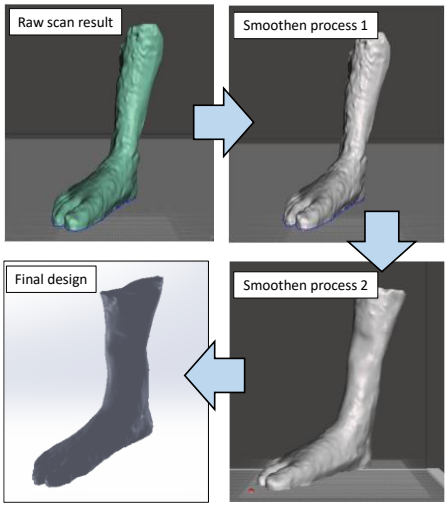

Figure 2. Meshmixer results

Figure 3. Measurement of real foot length is 22.7 cm

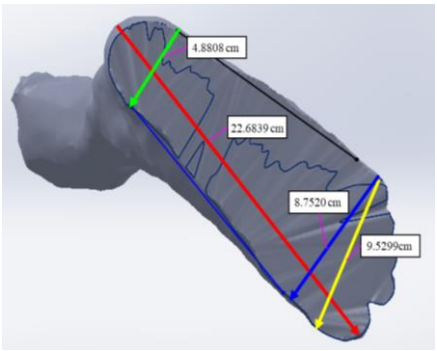

Figure 4. Adjusted foot length using SolidWorks

Meshmixer was utilized for preparing scanned lower limb model for 3D printing process. It exports the model into a format compatible with the 3D printers, such as STL. This software also provides several features which includes smoothening the surface of 3D model and converting it into SolidWorks file. The Meshmixer 3D scanned rendering result depicted in Figure 2. The 3D model is ready to be used for designing AFO. After converting into SolidWorks file, the measurement for the foot was scaled up. It turns out that discrepancies in the vertical dimension between the 3D-scanned foot and the patient's foot exist as depicted on Figure 3. The adjustment was made by scaling the size using SolidWorks software to ensure the optimal fit of AFO for the patient resulted in Figure 4. Once the 3D model and dimensions were generated, then the AFO design was performed. The scanning process result displays the detailed morphology of the patient's foot. Afterwards, the designing process of the AFO was conducted using SolidWorks based on the refined 3D scan result. The design was carried out by outlining the foot and calf structure presented. When the basic design of the AFO is completed, the 3D scan data is removed. Subsequently, AFO surface and edges are refined. Since the main focus of this project focused on fixing the angle of the foot, adding straps are essential to tighten the foot and the orthotics device. Hence, slots for strap placement were added to the design.

The final design of the AFO is depicted on Figure 5 which also divided into 6 parts for FEA purpose. The bottom part (Part 1) in contacts the sole which provides support from underneath while evenly distributing pressure. Part 2, the ankle support, wraps the lower back part of the leg (ankle) aiding in proper foot alignment. Extending further up the leg, Part 3, the lower calf support ensures that the orthotic remains correctly positioned during movement. Part 4 is the upper calf strap area, designed for attaching straps that wrap around the upper calf, securing the orthotic securely to the leg and preventing unwanted movement. Part 5 provides medial (inner) support to the foot and ankle maintaining proper alignment. Lastly, Part 6 provides lateral (outer) support, working in conjunction with the medial support to keep the foot and ankle stable and aligned. Hence, the FEA simulations were conducted on each part to analyze the performance of the design.

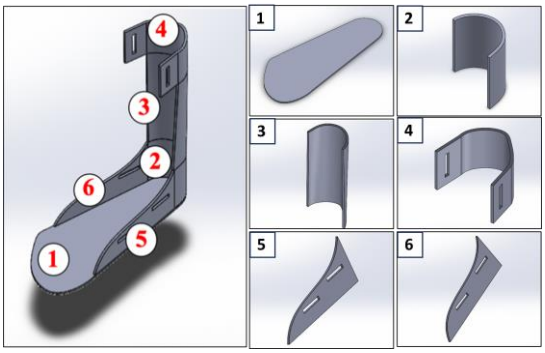

Figure 5. Final design with 3 mm design thickness divided into 6 parts, 1) bottom, 2) ankle, 3) lower calf, 4) upper calf, 5) medial, and 6) lateral supports.

Finite Element Analysis Result

The Finite Element Analysis which resulting in Von Mises Stress was calculated and shown in Figure 6 to Figure 11 and Table 1. It is particularly valuable in assessing the potential yielding or failure of the AFO material under complex loading conditions. It is employed to predict and analyze material failure or deformation under the mechanical loads applied to the object. Therefore, during the designing process, it ensures the specimen or prototype meets the safety and performance standard.

The direction of the force for each part varied depending on the contact surface of the components. Figure 6 illustrates the stress distribution in Part 1, the bottom support of the AFO, where the upper surface contacts the patient's sole. The body force is applied vertically to the top face of the component, while the bottom surface acts as the fixed support. The maximum and minimum stress occurs are 4.393×10^4 N/m^2 and 1.071×10^4 N/m^2, respectively. The color coding in the image illustrates the stress distribution, with blue indicating lower stress areas and red representing higher stress areas. It depicted that the edges exhibit higher stress compared to the center, highlighting areas that are more susceptible to deformation or failure.

For parts 2 to 4, the contact surfaces are located on the inner surfaces of each part. Forces act towards those inner surfaces of the components, with the opposite side providing fixed support. Thus, the simulation's boundary conditions of each part are identical. The critical points for each part mostly occur at the edges. On the lower leg support (see Figure 7), the highest stress value reaches 1.998×10^5 N/m², while the lowest is 3.283×10^4 N/m². In Figure 8, the lower calf part exhibits a maximum stress of 7.157×10^4 N/m² and a minimum of 1.372×10^4N/m². Moving up to the upper calf support on Figure 9 (part 4) the maximum and the maximum stress exhibit are 1.816×10^5 N/m² and 1.819 N/m², respectively. In this particular segment, the strap attachment area is found to experience the lowest stress compared to other parts since the tension from the strap is neglected. Besides, among all the three elements, the highest maximum stress developed in part 2 as the ankle support on Figure 9 as it reaches 1.998×10^5 N/m^2 or equal to 199.8 kPa.

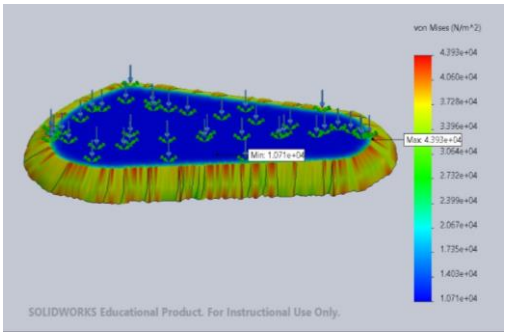

Figure 6. Finite Element Analysis Part 1, bottom support of The AFO Design

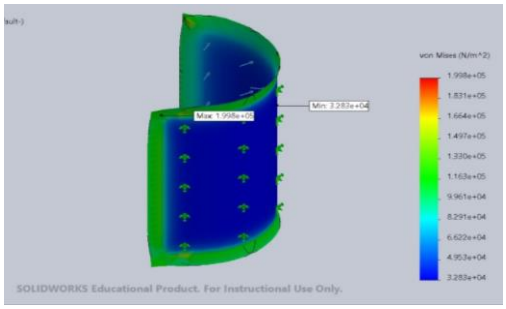

Figure 7. Finite Element Analysis Part 2, lower leg support of The AFO Design

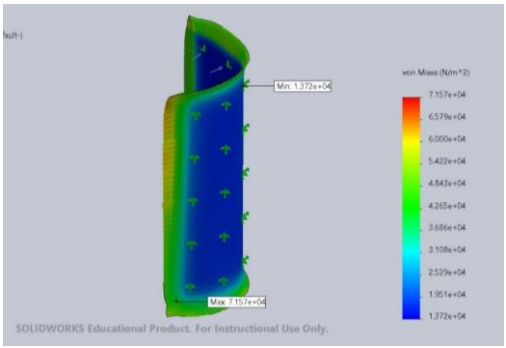

Figure 8. Finite Element Analysis Part 3, lower calf support of The AFO Design

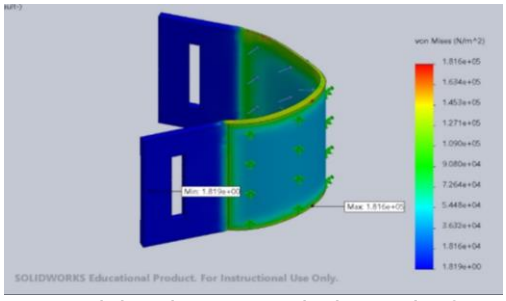

Figure 9. Finite element analysis result of part 4, upper calf support of the AFO design

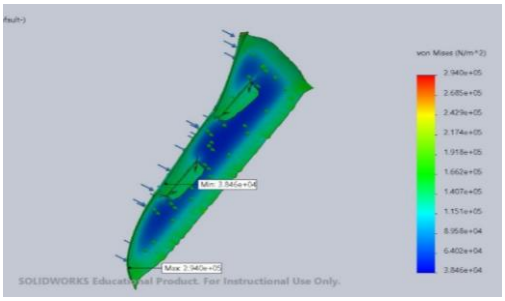

Figure 10. Finite element analysis of part 5, medial support of the AFO design

Figure 11. Finite element analysis of part 6, lateral support of the AFO design

For the last two components (Part 5 and 6), both components share an identical geometric profile which applied in different positions. Part 5 is positioned on the inner side of the foot as the medial support, closer to the midline of the body and aligned with the toes. Conversely, part 6 acts as the lateral support, placed on the outer side of the foot, opposite the medial support. Therefore, the direction of forces, contact surfaces, and fixed supports for these components act in opposing directions. The maximum stress presence on components 5 and 6 were found to be relatively high which are 2.940×10^5 N/m^2 and 2.477×10^5 N/m^2, respectively. The color code reveals that the central part of the ankle support shows lower stress values. In contrast, the edges exhibit higher stress values, making them more susceptible to deformation and potential failure. The details of the maximum and minimum von Mises stress analysis for each component were compiled and listed in Table 1. Among all components, Part 1 has the lowest von Mises stress, ranging from 10.71 to 43.93 kPa, indicating better stress distribution. Conversely, Part 5 experiences the highest minimum and maximum von Mises stress values, at 38.46 kPa and 294.0 kPa, respectively. These findings align with the study conducted by Totah et. al. [28], which used finite element analysis on an entire AFO made by the plaster casting method.

Their research also revealed similar critical stress concentrations in the ankle area, corresponding to Parts 4-6, and the lowest stress concentrations at the upper calf. On the other hand, the yield strength of pure polypropylene (PP) in room temperature stands at approximately 32-35 MPa [25]. Thus, based on the FEA results, all stress levels are below the specified yield strength of PP. This affirms that the design maximum stress concentration values occurred within an acceptable range, establishing the reliability of the AFO.

Prototype Fabrication Result

Upon completing the simulation procedure, the assembled prototype can be fabricated using FDM 3D printing. The printed AFO prototype is presented in Figure 12 (a). Additionally, various supplementary components are incorporated to ensure the specimen's functionality and suitability for testing purposes. The final assembly of the AFO is shown on Figure 12 (b).

Evaluation

a. Gait Cycle Analysis

The testing section conducted according to the normal gait cycle. The range of motion (ROM) of the ankle occurs primarily in the sagittal plane as the sum of plantar- and dorsiflexion angle. The ankle normal angle of the AFO is 90°. To validate reliability of the prototype, this study manually measures the angle of foot and calf as depicted on Figure 13. Notably, the observed angles of the testing result during gait cycle range from 89.7° to 105.8°. Hence, the maximum of dorsiflexion and plantar flexion is 0.3° (0.33%) and 15.8° (17.5%), respectively. It means that the sum of dorsiflexion and plantar flexion angle is 16.1° which comparable the ROM values of AFO gait cycle analysis from previous study (10°–16°) [29]. Moreover, during everyday activities, the maximum ROM in the sagittal plane is 30° for walking [27]. Thus, the AFO fabricated in this study found to be reliable since the ROM angle lays within the acceptable range.

Table 1. Result of Von Mises Stress Analysis Using SolidWorks

Symbol	Von Mises Stress	
	Min	Max
1	10.71 kPa	43.93 kPa
2	32.83 kPa	199.8 kPa
3	13.72 kPa	71.57 kPa
4	18.19 kPa	181.6 kPa
5	38.46 kPa	294.0 kPa
6	33.24 kPa	247.7 kPa

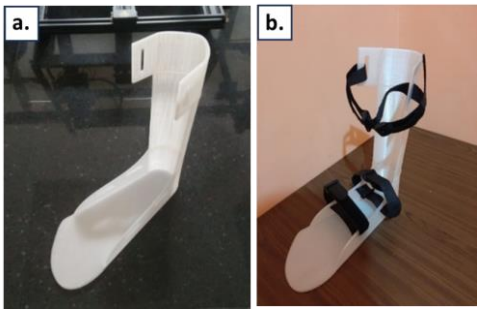

Figure 12. (a) 3D printed AFO using FDM and PP material (b) AFO prototype after assembly

b. Time Effectiveness Analysis

The main purpose of this study is to compare conventional, and 3D printed AFO based on the amount of production time. The comparison between conventional and 3D printed AFO can be seen in Figure 14. According to R.K. Chen et. al. [30] the process of conventional manufacturing involves more production time compared to the 3D printing process. As conventional AFO is typically produced using traditional fabrication methods, it requires several manufacturing processes which involve shaping materials like plastic or metal based on a cast of the patient's limb. The process took longer time, approximately 126.5 hours since it involves measurement of negative impression size which then converted into positive mode using gypsum mixture. Additionally, the finishing stage is required which manually executed using sandpaper etc. Conversely, 3D printing methods promote shorter production time compared to the traditional one. It only required several simple steps such as measurement stage, capture the limb photo for scanning, rendering the image, then followed by design and analysis. Lastly the, after all the stages are completed, it comes to the last part which is 3D printing process. Based on the duration calculations, it only takes 38 hours to complete which saves approximately 70% of the conventional one.

In comparison with previous research, the current study's approach to developing an Ankle Foot Orthotics (AFO) device using 3D scanning and printing methods presents notable advancements in accuracy, and efficiency. The FEA results confirmed the findings of Totah et al. [27], which highlighted similar critical stress concentrations in the ankle area. This agreement underscores the reliability of the present study's methodology and its alignment with past research. Furthermore, the prototype fabrication using FDM 3D printing demonstrated a significant reduction in production time compared to conventional methods, supporting the observations made by Chen et al. [29]. The 3D printed AFO was produced in approximately 38 hours, saving around 70% of the time required for traditional fabrication.

Moreover, the gait cycle analysis revealed that the AFO prototype provided an acceptable range of motion, consistent with values reported in previous studies, thus validating the functional performance of the design. The observed dorsiflexion and plantar flexion angles fell within the normal range, ensuring that the AFO supports natural gait patterns without compromising mobility. In summary, the integration of advanced 3D technologies in the design and production of AFOs offers substantial improvements in terms of precision, efficiency, and reliability. The findings of this study highlight the potential for these technologies to revolutionize the field of orthotics, providing better outcomes for patients through more accurate and faster production of custom AFO devices.

Figure 13. Angle of ankle based on the Gait cycle

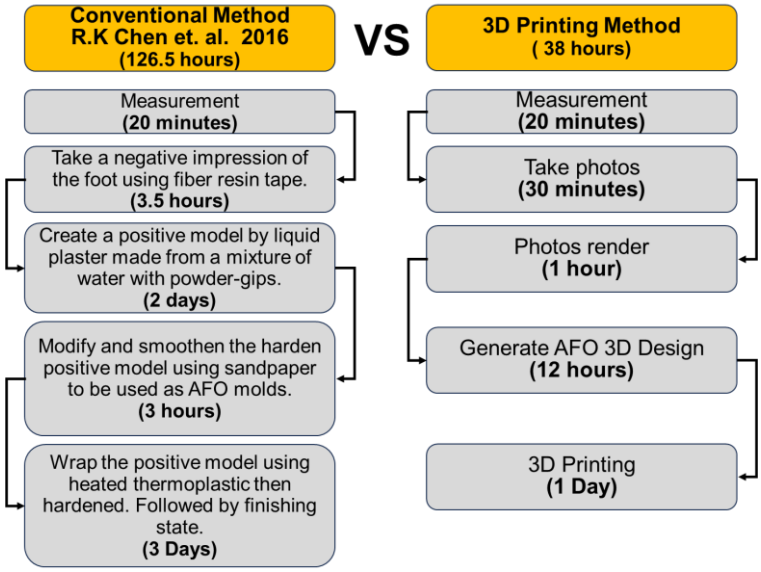

Figure 14. Comparison of the production time for conventional manufacturing vs proposed 3D printing method

CONCLUSION

The primary objective of this study has been achieved by successfully implementing photogrammetry scanning method using 3DF Zephyr, as a time-effective alternative method for constructing Ankle-Foot Orthotics (AFOs) design. This paper also proves that the 3D scan method employed within this research successfully produced the required AFO based on digitized data from photos. It was fabricated through FDM printing with PP material, and the 3D model was created by using mainly three software which are 3D Zephyr, Meshmixer, and SolidWorks. The implementation of photogrammetry has demonstrated remarkable success in generating accurate dimensions of 3D models. During the gait cycle, the ROM values of the AFO is 16.1 degrees which is in the acceptable standard range of motion for walking gait cycle. Moreover, this study marks a notable advancement in orthotic design by introducing a time-efficient approach. It contributed to a significant reduction of 70% in the overall time required for conventional AFO fabrication. Therefore, the AFOs produced through this methodology exhibit promising efficacy.

REFERENCES

[1] D. C. Suárez and L. Cameron, “10 Disability in Indonesia: What can we learn from the available data?,” in *In Sickness and In Health*, F. Witoelar and A. Utomo, Eds., ISEAS–Yusof Ishak Institute Singapore, 2022, pp. 172–200. doi: 10.1355/9789815011852-015.

[2] T. Sarma, K. Kumar Saxena, V. Majhi, D. Pandey, R. Prakash Tewari, and N. Sahai, “Development of active ankle foot orthotic device,” *Materials Today: Proceedings*, vol. 26, pp. 918–921, 2020, doi: 10.1016/j.matpr.2020.01.143.

[3] L. Y. Yeung and K. Subburaj, “3D-printed orthotics for pediatric lower limb deformities correction,” in *3D Printing in Podiatric Medicine*, Elsevier, 2023, pp. 51–81. doi: 10.1016/B978-0-323-91911-1.00003-1.

[4] P. Caravaggi *et al.*, “Functional evaluation of a novel fibreglass-reinforced polyamide custom dynamic AFO for foot drop patients: A pilot study,” *Gait & Posture*, vol. 109, pp. 41–48, Mar. 2024, doi: 10.1016/j.gaitpost. 2024.01.017.

[5] M. A. Laribi and S. Zeghloul, “Human lower limb operation tracking via motion capture systems,” in *Design and Operation of Human Locomotion Systems*, Elsevier, 2020, pp. 83–107. doi: 10.1016/B978-0-12-815659-9.00004-4.

[6] A. Nouri, L. Wang, Y. Li, and C. Wen, “Materials and Manufacturing for Ankle–Foot Orthoses: A Review,” *Advanced Engineering Materials*, vol. 25, no. 20, p. 2300238, Oct. 2023, doi: 10.1002/adem. 202300238.

[7] J. Barrios-Muriel, F. Romero-Sánchez, F. J. Alonso-Sánchez, and D. Rodríguez Salgado, “Advances in Orthotic and Prosthetic Manufacturing: A Technology Review,” *Materials*, vol. 13, no. 2, p. 295, Jan. 2020, doi: 10.3390/ma13020295.

[8] K. J. Walker *et al.*, “Novel 3D-printed foot orthoses with variable hardness: A comfort

comparison to traditional orthoses," *Medical Engineering & Physics*, vol. 115, p. 103978, May 2023, doi: 10.1016/j.medengphy.2023. 103978.

[9] M. Farhan, J. Z. Wang, P. Bray, J. Burns, and T. L. Cheng, "Comparison of 3D scanning versus traditional methods of capturing foot and ankle morphology for the fabrication of orthoses: a systematic review," *Journal of Foot and Ankle Research*, vol. 14, no. 1, p. 2, Dec. 2021, doi: 10.1186/s13047-020-00442-8.

[10] A. J. Octarina, K. Saptaji, and T. Kurniawan, "Optimization of relative density to geometric parameter ratio for honeycomb structure using Finite Element Analysis," *IOP Conference Series: Materials Science and Engineering*, vol. 1098, no. 6, p. 062102, Mar. 2021, doi: 10.1088/1757-899X/1098/6/062102.

[11] A. Sharma and A. Rai, "Fused deposition modelling (FDM) based 3D & 4D Printing: A state of art review," *Materials Today: Proceedings*, vol. 62, pp. 367–372, 2022, doi: 10.1016/j.matpr.2022.03.679.

[12] A. Asriyanti *et al.*, "Fabrication of Rigid Polyurethane Foam Lumbar Spine Model for Surgical Training using Indirect Additive Manufacturing," *International Journal of Technology*, vol. 13, no. 8, p. 1612, Dec. 2022, doi: 10.14716/ijtech.v13i8.6125.

[13] M. Bragaglia, F. Cecchini, L. Paleari, M. Ferrara, M. Rinaldi, and F. Nanni, "Modeling the fracture behavior of 3D-printed PLA as a laminate composite: Influence of printing parameters on failure and mechanical properties," *Composite Structures*, vol. 322, p. 117379, Oct. 2023, doi: 10.1016/j.compstruct.2023.117379.

[14] D. Anand, O. I. Khalaf, F. Hajjej, W.-K. Wong, S.-H. Pan, and G. R. Chandra, "Optimized Swarm Enabled Deep Learning Technique for Bone Tumor Detection using Histopathological Image," *SINERGI*, vol. 27, no. 3, p. 451, Sep. 2023, doi: 10.22441/sinergi.2023.3.016.

[15] A. Bugeja, M. Bonanno, and L. Garg, "3D scanning in the art & design industry," *Materials Today: Proceedings*, vol. 63, pp. 718–725, 2022, doi: 10.1016/j.matpr.2022. 05.069.

[16] K. Chhikara, G. Singh, S. Gupta, and A. Chanda, "Progress of additive manufacturing in fabrication of foot orthoses for diabetic patients: A review," *Annals of 3D Printed Medicine*, vol. 8, p. 100085, Oct. 2022, doi: 10.1016/j.stlm. 2022.100085.

[17] M. Javaid, A. Haleem, R. P. Singh, and R. Suman, "3D printing applications for healthcare research and development," *Global Health Journal*, vol. 6, no. 4, pp. 217–226, Dec. 2022, doi: 10.1016/j.glohj. 2022.11.001.

[18] A. Sastranegara, K. Eka Putra, E. Halawa, N. A. Sutisna, and A. Topa, "Finite Element Analysis on ballistic impact performance of multi-layered bulletproof vest impacted by 9 mm bullet," *SINERGI*, vol. 27, no. 1, p. 15, Jan. 2023, doi: 10.22441/sinergi.2023.1. 003.

[19] S. F. Moula, S. T. Sporsho, N. A. Chanda, and M. D. Xames, "Design and Development of a Multifunctional Convertible Wheelchair in a Low-Income Country Context," *Indonesian Journal of Computing, Engineering and Design (IJoCED)*, vol. 5, no. 1, p. 8, Apr. 2023, doi: 10.35806/ijoced.v5i1.304.

[20] Md. H. Ali, Z. Smagulov, and T. Otepbergenov, "Finite element analysis of the CFRP-based 3D printed ankle-foot orthosis," *Procedia Computer Science*, vol. 179, pp. 55–62, 2021, doi: 10.1016/j.procs.2020.12.008.

[21] K. Saptaji, A. A. Sholeh, G. Priyandoko, and I. B. Hadisujoto, "Development of Electric Discharge Machining (EDM) using Solenoid Actuator for Educational Purpose," *SINERGI*, vol. 25, no. 3, p. 279, Jul. 2021, doi: 10.22441/sinergi.2021.3. 005.

[22] H. K. Surmen and Y. Z. Arslan, "Evaluation of various design concepts in passive ankle-foot orthoses using finite element analysis," *Engineering Science and Technology, an International Journal*, vol. 24, no. 6, pp. 1301–1307, Dec. 2021, doi: 10.1016/j.jestch.2021.03.004.

[23] A. B. Prasetiyo and K. A. Sekarjati, "Finite Element Simulation of Power Weeder Machine Frame," *Indonesian Journal of Computing, Engineering and Design (IJoCED)*, vol. 4, no. 2, p. 25, Oct. 2022, doi: 10.35806/ijoced.v4i2.291.

[24] N. E. Zander, M. Gillan, Z. Burckhard, and F. Gardea, "Recycled polypropylene blends as novel 3D printing materials," *Additive Manufacturing*, vol. 25, pp. 122–130, Jan. 2019, doi: 10.1016/j.addma.2018.11.009.

[25] F. T. Jahromi, M. Nikzad, M. Isaksson, and J. Norén, "Mechanical properties of 3D-printed staking polypropylene posts for repairing automotive headlights," *The International Journal of Advanced Manufacturing Technology*, vol. 127, no. 11–

12, pp. 5553–5567, Aug. 2023, doi: 10.1007/s00170-023-11891-3.
[26] S. M. H. Sithi Shameem Fathima, K. A. Jyotsna, T. Srinivasulu, K. Archana, M. Tulasi Rama, and S. Ravichand, "Walking pattern analysis using GAIT cycles and silhouettes for clinical applications," *Measurement: Sensors*, vol. 30, p. 100893, Dec. 2023, doi: 10.1016/j.measen.2023. 100893.
[27] J. Block, S. Faller, D. Heitzmann, M. Alimusaj, and S. I. Wolf, "Using the ankle as the knee –range of motion in adults following rotation-plasty ((Borggreve/ Van Nes))," *Gait & Posture*, vol. 97, pp. S371–S372, Sep. 2022, doi: 10.1016/j.gaitpost. 2022.07.222.
[28] D. Totah, I. Kovalenko, M. Saez, and K. Barton, "Manufacturing Choices for Ankle-Foot Orthoses: A Multi-objective Optimization," *Procedia CIRP*, vol. 65, pp. 145–150, 2017, doi: 10.1016/j.procir.2017. 04.014.
[29] K. Watanabe, A. Teramoto, T. Kamiya, Y. Okada, Y. Murahashi, and T. Yamashita, "A Comparative Study of Foot Range of Motion and Activities of Daily Living Status of Patients Following Ankle Arthrodesis and Tibiotalocalcaneal Arthrodesis," *The Journal of Foot and Ankle Surgery*, vol. 62, no. 3, pp. 519–523, May 2023, doi: 10.1053/j.jfas.2022.12.007.
[30] R. K. Chen, Y. Jin, J. Wensman, and A. Shih, "Additive manufacturing of custom orthoses and prostheses—A review," *Additive Manufacturing*, vol. 12, pp. 77–89, Oct. 2016, doi: 10.1016/j.addma.2016. 04.002.